Communication

Vladimir I. Kukulin, Anton V. Bibikov, Eugene V. Tkalya, Matteo Ceccarelli, Igor V. Bodrenko*

^{7}Be and ^{22}Na radionuclides for a new therapy for cancer

https://doi.org/10.1515/bmc-2022-0028
received February 2, 2023; accepted April 18, 2023

Abstract: ^{10}B isotopes have been almost exclusively used in the neutron-capture radiation therapy (NCT) of cancer for decades. We have identified two other nuclides suitable for radiotherapy, which have ca. ten times larger cross section of absorption for neutrons and emit heavy charged particles. This would provide several key advantages for potential NCT, such as the possibility to use a lower nuclide concentration in the target tissues or a lower neutron irradiation flux. By detecting the characteristic γ radiation from the spontaneous decay of the radionuclides, one can image their biodistribution. These advantages could open up new possibilities for NCT applications as a safer and more efficient cancer therapy.

Keywords: radiotherapy, neutron capture, radionuclides, theranostics

Introduction

The use of ionizing radiation in cancer therapy has a long and successful history [1,2]. It is one of the most remarkable examples of direct medical application of the results of modern physics utilized in more than 50% of patients with cancer [3].

The ionizing radiation can be delivered from outside the patient, a method known as external-beam radiation therapy (EBRT). Heavy charged particles (protons, accelerated nuclei) have an advantage over leptons and photons due to relatively small range straggling and to the sharp Bragg peak in the energy loss vs the path length curve, located at the end of the particle's range in the tissue [4–6]. To access tumors located deep in the body, one needs to accelerate the particles up to the energies of a few hundred MeV/nucleon and to focus the beam onto the target in the human body. This makes the infrastructure for heavy particle radiation therapy very complex, expensive, and limited to large medical/research centers, while a much cheaper γ-ray radiation therapy has come to many common hospitals [5,7].

Alternatively, one may use radioactive nuclides bound into radiopharmaceuticals and selectively transported into the target tissues [8]. The spontaneous decay of a radioactive nucleus may release up to several tens of MeV, converted into the kinetic energy of charged particles producing the ionization within less than a millimeter range. The radionuclide therapy, therefore, replaces the problem of kinematic delivery of the ionizing particle into the target tissue in EBRT with the problem of selective accumulation of radiopharmaceuticals. The radionuclide therapy also brings a new issue – the problematic temporal control. The timescales of the accumulation and of the excretion of the radiopharmaceuticals (which are regulated by the metabolism and are difficult to control) should be in due relation to the lifetime of the isotope so that to maximize the part of the nuclei decayed in the tumor and not on their way into or out of the target.

In neutron capture radiation therapy (NCT), the active isotope undergoes induced radioactive decay following the capture of a neutron. This method combines the local energy deposition properties of the radionuclide therapy and a good temporal control of the beam particle radiation therapy, as the neutron flux may be switched on and off quickly. The idea was suggested in 1936 [9] and then implemented for the first time in 1954 [10] by utilizing the ^{10}B

*** Corresponding author: Igor V. Bodrenko,** Istituto Officina dei Materiali, CNR-IOM Cagliari, Cittadella Universitaria, Monserrato (CA) 09042-I, Italy; Ecole Normale Sup´erieure, D´epartement de Chimie – Laboratoire PASTEUR, 24 Rue Lhomond, 75005 Paris, France, e-mail: igor.bodrenko@cnr.it
Vladimir I. Kukulin, Anton V. Bibikov: Skobeltsyn Institute of Nuclear Physics, Lomonosov Moscow State University, Leninskie gory, Moscow, Ru-119991, Russia
Eugene V. Tkalya: P.N. Lebedev Physical Institute of the Russian Academy of Sciences, 119991, 53 Leninskiy pr., Moscow, Russia; Nuclear Safety Institute of RAS, Bol'shaya Tulskaya 52, Moscow, 115191, Russia
Matteo Ceccarelli: Department of Physics, University of Cagliari, S.P. Monserrato-Sestu km 0.700, I-09042 Monserrato (CA), Italy; Istituto Officina dei Materiali, CNR-IOM Cagliari, Cittadella Universitaria, Monserrato (CA) 09042-I, Italy, e-mail: matteo.ceccarelli@dsf.unica.it

isotope and the reaction $^{10}B(n,\alpha\gamma)^{7}Li$. However, despite more than 60 years of research and development, boron neutron capture therapy (BNCT) is still in the experimental phase [11–14]. Several issues are cited as the reason for this situation [15]. First, it is often difficult to identify boron-containing compounds that can be selectively accumulated and kept at the necessary concentration in specific tumor cells. Second, besides many successful practical applications, a significant number of adverse side effects due to neutron irradiation of healthy tissues were observed. Third, relatively high neutron fluxes (10^{9}–10^{10} cm^{-2} s^{-1}) required by the BNCT were available only in nuclear reactors and in large-scale accelerator complexes until recently, thus assuming an infrastructure that is complex, expensive, and not well suited for systematic clinical studies.

The only alternative up to date, gadolinium, in particular, the ^{157}Gd isotope (GdNCT) in the reaction $^{157}Gd(n,\gamma)^{158}Gd$, has been considered for NCT, although to a much lesser extent [16]. The main advantage of the GdNCT, its huge cross section of thermal neutron absorption (by more than 60 times larger than that for ^{10}B), is diminished by the fact that in most cases the $^{158}Gd^{*}$ excitation energy is taken away from the target tissues by high-energy γ photons, which do not create any local ionization. On average, only a small part of the excitation energy (less than 1%) is radiated in the form of electrons via the internal conversion and Auger mechanisms, which produce ionization within a 0.1 mm range from the source [17]. As a result, GdNCT has no obvious benefits over BNCT and still remains in the experimental phase, mostly focused on the identification of appropriate tumor-selective Gd delivery agents or hybrid B–Gd-containing compounds [18].

Presently, due to the recent developments of compact accelerators for neutron production, there is a growing interest in NCT worldwide [15,19]. The therapy is available in hospital-based facilities, and there is a strong need for novel drugs, which makes this topic extremely hot. In this work, we have identified two new nuclides, ^{7}Be and ^{22}Na, suitable for radiation therapy and analyzed their capabilities to serve in novel NCTs.

Experimental background and estimates

Nuclide properties

Both ^{7}Be and ^{22}Na are unstable radionuclides (Figure 1) and are well-known to physicists. ^{7}Be decays into stable ^{7}Li via the electron capture mechanism with a half-life of 53 days. As the decay rate depends on the electronic density at the nucleus, ^{7}Be has been used to study the effects of the chemical environment in the nuclear processes [22–24]. More importantly, ^{7}Be is assumed to play a key role in the lithium yield of the big-bang nucleosynthesis for standard cosmology via the neutron absorption reaction $^{7}Be(n,p)^{7}Li$ [25,26]. ^{22}Na decays mainly by emitting positrons and γ-radiation into a stable ^{22}Ne isotope and has a half-life of 2.6 years. It is important for the nucleosynthesis problem [27] and also is used in positron emission tomography (PET).

In Figure 2 and Table 1, we summarize the neutron capture properties of the two radionuclides and compare them with those of ^{10}B. The neutron capture reactions pass via an intermediate compound nucleus in an excited state –

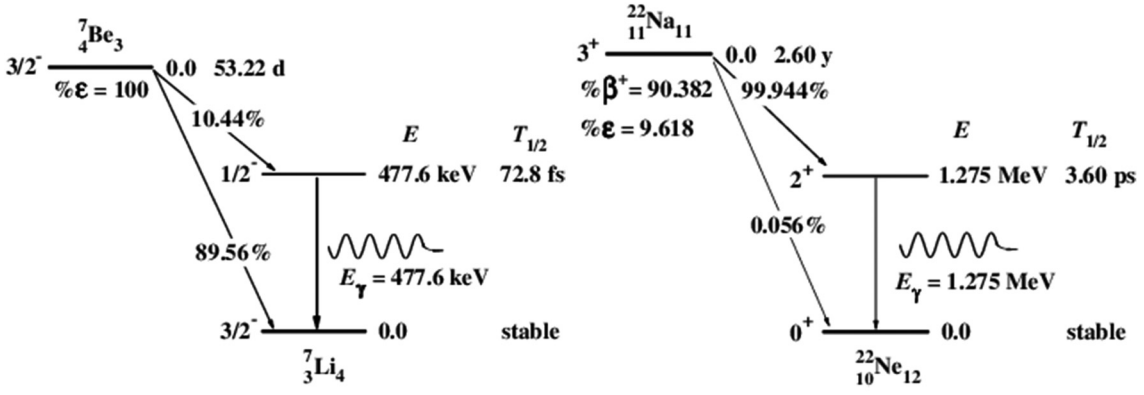

Figure 1: Schematic diagrams of ^{7}Be (a) and ^{22}Na (b) spontaneous decay; the data are from Tilley et al. [20] and Basunia [21], respectively.

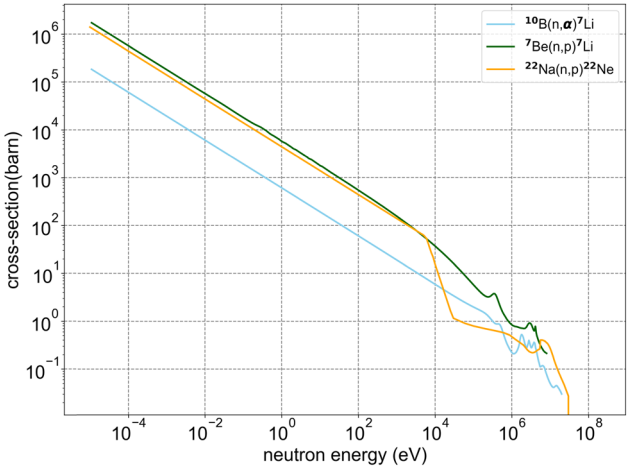

Figure 2: Neutron absorption cross section for NCT-related reactions [28].

^{11}B, ^{8}Be, or ^{23}Na. The compound nuclei then decay into the daughter nuclei (^{7}Li in the case of B and Be and ^{22}Ne for Na) by emitting a heavy particle – an α-particle for boron and a proton for beryllium and sodium. With a probability of 93.3%, ^{11}B* decays into the first excited state of ^{7}Li emitting the characteristic 478 keV γ-radiation (Figure 1a). Also, ^{23}Na* decays mainly (99.15%) into the first excited state of its daughter nucleus, ^{22}Ne, emitting the 1.275 MeV photon (Figure 1b). In contrast, ^{8}Be* decays predominantly (98.8%) into the ground state of ^{7}Li. The cross section for the ^{10}B (n,αγ)^{7}Li reaction is well determined (see the recent update in the study of Carlson et al. [29]). It follows Bethe's ∝ 1/v law with an accuracy better than 5% for the neutron incident energies E_n < 100 keV so that $\sigma_{n\alpha}\sqrt{E_n}$ = 0.6114 kb eV$^{1/2}$. The cross section of ^{7}Be(n,p)^{7}Li follows the ∝ 1/v law for a much smaller neutron kinetic energy range, E_n < 100 eV [26]. Moreover, there is inconsistency (of more than 20%) between the $\sigma_{n\alpha}$ values obtained by different research groups. Thus, for the thermal neutrons (E_n = 0.0253 eV) the neutron capture cross section varies from 38.4 ± 0.8 kb [31] to 52.3 ± 5.2 kb [26]. This discrepancy is still under debate [30]. We have adopted the latest result [30] so that $\sigma_{n\alpha}\sqrt{E_n}$ = 7.0 kb eV$^{1/2}$ in the abovementioned neutron energy range. The ^{22}Na(n,pγ)^{22}Ne reaction also follows the ∝ 1/v law until the neutron energies, E_n < 100 eV, so that $\sigma_{n\alpha}\sqrt{E_n}$ = 5.0 kb eV$^{1/2}$ [27].

It is interesting to note that, besides ^{7}Be and ^{22}Na, there are no other reasonably stable nuclides that have the capture cross section for the thermal and the epithermal neutrons larger than that for ^{10}B and emit high linear energy transfer (LET) radiation [29]. There are very strong neutron absorbers like ^{135}Xe and ^{113}Cd but via the (n, γ) reaction, i.e., emitting γ-radiation is not suitable for the NCT.

Neutron capture energy deposition

For a more direct comparison of the BNCT with potential BeNCT and NaNCT, we have estimated the energy deposition after neutron capture in water (Table 2), considering only the predominant reaction channels. The γ-radiation

Table 1: Neutron capture properties [27,29,30]

Nuclide properties		
^{10}B(J^{π} = 3^{+}) stable	$^{7}\mathrm{Be}\left(\frac{3^-}{2}\right) \xrightarrow{53.2\ \mathrm{d}} {}^{7}\mathrm{Li}$	$^{22}\mathrm{Na}(3^+) \xrightarrow{2.60\ \mathrm{y}} {}^{22}\mathrm{Ne}$
Main reaction channels: "0" – the ground state of the daughter nucleus; "1" – the first excited state		
^{10}B + n → ^{11}B* →	^{7}Be + n → ^{8}Be* →	^{22}Na + n → ^{23}Na* →
(93.3%) ^{7}Li$_1$ + α$_1$ + γ	(1.2%) ^{7}Li$_1$ + p$_1$ + γ	(99.15%) ^{22}Ne$_1$ + p$_1$ + γ
(6.7%) ^{7}Li$_0$ + α$_0$	(98.8%) ^{7}Li$_0$ + p$_0$	(0.85%) ^{22}Ne$_0$ + p$_0$
Kinetic energy of heavy particle products in the predominant channel [MeV]		
0.84(^{7}Li$_1$) + 1.47(α$_1$)	0.21(^{7}Li$_0$) + 1.44(p$_0$)	0.10(^{22}Ne$_1$) + 2.25(p$_1$)
Total neutron capture cross section $\sigma_{nx}\sqrt{E_n}$ [kb eV$^{1/2}$]		
0.6114	7.0	5.0
***σ_{nx}* (E_n [eV]) [kb]**		
$\sigma_{n\alpha}$ (0.0253) = 3.844	σ_{np} (0.0253) = 44	σ_{np} (0.0253) = 31
$\sigma_{n\alpha}$ (1.0) = 0.611	σ_{np} (1.0) = 7.0	σ_{np} (1.0) = 5.0
$\sigma_{n\alpha}$ (10) = 0.193	σ_{np} (10) = 2.2	σ_{np} (10) = 1.6
$\sigma_{n\alpha}$ (100) = 0.0611	σ_{np} (100) = 0.7	σ_{np} (100) = 0.5

Table 2: BNCT (left) vs BeNCT (center) vs NaNCT (right): the energy deposition in water

High LET radiation energy, E_t [MeV]		
2.31	1.65	2.35
Ranges [μm] of the high LET radiation [32,33]		
R_α = 8, R_{Li} = 5	R_p = 44 , R_{Li} = 2	R_p = 92, R_{Ne} < 1
Number of reactions per cell (N_r) required for a dose of 20 Gy		
120	170	120
Nuclide concentration, $c(E_n)$ [μg g^{-1}] (in parenthesis – the number of nuclides per cell, $N_{cell}(E_n)$) required for a dose of 20 Gy absorbed during 1 h exposition to neutron flux of 10^{10} s^{-1} cm^{-2}		
	E_n = 0.0253 eV	
6.5 (0.9 × 10^9)	0.56 (0.11 × 10^9)	1.7 (0.11 × 10^9)
	E_n = 1.0 eV	
41 (5.7 × 10^9)	3.5 (0.69 × 10^9)	11 (0.68 × 10^9)
	E_n = 10.0 eV	
130 (18 × 10^9)	11 (2.2 × 10^9)	34 (2.1 × 10^9)
	E_n = 100.0 eV	
410 (57 × 10^9)	35 (6.9 × 10^9)	110 (6.8 × 10^9)

The values "per cell" stand for per mass, M_{cell} = 2.3 ng; and E_n denotes the neutron kinetic energy.

emitted in the predominant channels for BNCT and NaNCT (Table 1) is a low LET radiation. This type of radiation has a low probability to produce ionization in the vicinity of the decaying nuclide but it rather escapes from the tumor region. A part of the decay energy may be transformed into the electronic excitation of the daughter nucleus via different mechanisms (e.g., the internal conversion, the coulomb excitation by the emitting charged particles, the shake-off due to the instant change in the nucleus charge, and of its momentum) and can be released in the form of Auger electrons and photons. However, for the light elements considered here (Be, B, and Na), the energy released in this form and its biological effects may probably be neglected for the NCT, in contrast with the heavy elements like Gd, where internal conversion is important [17]. Thus, only the kinetic energy, E_t, transferred to charged heavy particles (high LET radiation) is useful for the NCT and is reported at the top of Table 2.

To relate the radiation doses in water in the biological context, we will consider a typical cell linear dimension, L_{cell} = 13 μm, and a typical cell mass, M_{cell} = 2.3 ng; see Appendix A. Also, we will assume D_t = 20 Gy in tumor tissues for a typical dose required for the NCT in a single run [5,11]. To compare the nuclides, we use the number of neutron capture reactions per cell N_r, required to release locally the absorbed radiation dose D_t (see Appendix B). This quantity is independent of the neutron capture probability and reflects only the difference (among the nuclides) in the total energy of high LET radiation following the neutron capture. Only a part of the nuclides in the cell absorbs neutrons and contributes to the radiation dose, depending on the neutron flux, Φ_n, the neutron kinetic energy, E_n, the absorption cross section, σ_n (E_n), and the time of the irradiation. Therefore, the required number, N_{cell}, of nuclides per cell to give the absorbed dose D while exposing the cell for time t to neutron flux Φ_n is a more relevant quantity to compare NCT properties of nuclides. Alternatively to N_{cell}, the relative concentration, c, of the nuclide in the target (in the units of ppm or μg of the nuclide per 1 g of tissue) is often used. Both N_{cell} and c are shown in Table 2 for D_t = 20 Gy, t = 1 h, Φ_n = 10^{10} s^{-1} cm^{-2}, and for different neutron kinetic energies.

Discussion

BeNCT and NaNCT: advantage and perspective

Based on the data and the estimates shown in the tables, we can discuss the pros and cons of the potential BeNCT and NaNCT in comparison to the existing BNCT. First, the neutron absorption cross section for ^{7}Be is more than ten times (Table 1) larger, and for ^{22}Na it is more than eight times larger than that for ^{10}B for E_n < 100 eV. This principal advantage of the ^{7}Be is somewhat counterbalanced by a lower (by 30%) released kinetic energy of the high LET radiation (Table 2). For ^{22}Na, the kinetic energy release is almost the same as for ^{10}B. In the end, the required number of ^{7}Be nuclides per cell, N_{cell}, is the same as for ^{22}Na, and it is at least eight times smaller than that for the boron, at the same neutron flux and the exposition time. For example, for thermal neutrons, one would need 0.9 × 10^{9} ^{10}B nuclei per 2.3 ng of water (typical cell) to obtain 20 Gy of the absorbed radiation dose after 1 h of exposition to Φ_n = 10^{10} s^{-1} cm^{-2} neutron flux, while only 1.1 × 10^{8} of ^{7}Be or ^{22}Na is required. This ratio remains valid for neutron kinetic energies lower than 100 eV. As the requirement of sufficient concentration of the nuclide is one of the key issues in BNCT [14], the reduction by a factor of 8 in the case of ^{7}Be and of ^{22}Na may be crucial for the success of the NCT. The larger cross section would also make it possible to bring the required dose to the tumors more deeply buried in the body than for BNCT, thus increasing the potential applicability of the therapy.

The main ionizing particles are different for the boron and the new nuclides (α particles and protons, respectively), so the biological effect may be different at the same total kinetic energy. On the one hand, the α-particle has a shorter range and, if ^{10}B is located close to the cell nucleus, it will release its kinetic energy within several microns, creating maximum radiation damage directly to the DNA. The proton radiated by ^{7}Be or ^{22}Na after the neutron capture travels tens of microns and deposits its kinetic energy in several cells, thus reducing the biological damage to each one of them. On the other hand, if the activated nuclide is located in the cell far from the nucleus, the α-particle can stop before reaching the important organelles and produce only a small radiation damage. The proton, however, has a higher probability to hit a cell nucleus while crossing several adjacent cells and also delivers a more uniform dose in the areas containing the radionuclides, than in the case of ^{10}B. The abovementioned contributions that dominate the biological effect of the NCT will also depend on the mode the nuclide is accumulated inside the tumor cells. This is one key question for future experimental studies; it remains to be verified how much is the actual relative biological effect value of the protons compared to that of the α particles emitted in the reaction on ^{10}B.

Another way to profit from the larger neutron capture cross section for the new nuclides is to reduce the intensity

of neutron flux, again by a factor of 8, while keeping the nuclide concentration in the tumor the same as for ^{10}B. This will give two advantages to the BeNCT and the NaNCT. First, the probability of activation of the atomic nuclei (also other than Na and Be) as well as of the elastic and inelastic collisions of neutrons in the healthy tissues will be eight times smaller compared to BNCT, thus reducing the neutron irradiation adverse effects (it is assumed that the ratio of the nuclide concentrations in the tumor and in healthy tissues are not smaller than for BNCT). This is especially important, e.g., for the brain glioblastoma where the tumor is embedded deeply inside the brain tissue [12,34]. One needs to apply epithermal neutrons to reach the tumor in this case, and so any significant reduction of the neutron flux would be very beneficial. Second, a lower required intensity (10^{8-9} s^{-1} cm^{-2}) of the neutron beam would make it possible to use a smaller scale and cheaper accelerator-based neutron sources [35,36]. This would make the NCT economically more efficient and more competitive.

Additionally, as the reaction byproducts, the positrons from the spontaneous decay of ^{22}Na can be used in PET. The same holds for the characteristic γ-radiation (478 keV) from the spontaneous decay of ^{7}Be (Figure 1a) and the γ (1.28 MeV) from the spontaneous decay of ^{22}Na (Figure 1b), which can be utilized very favorably in the standard single photon emission computer tomography (SPECT) [37] to trace the biodistribution of the nuclide before neutron irradiation. This is also an important advantage over the BNCT, where the control of the nuclide accumulation is difficult, and one has to additionally label the boron-containing compound with ^{18}F to utilize PET [38].

Open problems

There are also new challenges in the way of ^{7}Be and ^{22}Na to the successful NCT management. ^{22}Na is used for PET and it is already a commercial product. On the 10–1,000 ng scale necessary for experimental studies, ^{7}Be may be produced as a byproduct on existing accelerator-based neutron sources utilizing, e.g., the proton-induced spallation reaction on ^{16}O [39]. For potential industrial-scale application, a dedicated production infrastructure will be necessary. In this respect, the idea (first suggested in Ref. [40]) of an accelerator for NCT utilizing the reverse reaction, ^{7}Li(p,n)^{7}Be, and an intense (10 mA and more) proton beam to produce neutrons looks especially attractive. Here, the beryllium isotope made during neutron generation can be further utilized for BeNCT, thus also reducing the cost of radioactive waste.

The radiotoxicity problem of these radioactive isotopes is another one. That is, one has to understand and minimize the adverse effects of the spontaneous radiation on the patient, but also on his/her family, the personnel, and the environment during drug production, administration, excretion, and radioactive waste management. To assess the effects of the spontaneous radiation of the ^{7}Be and the ^{22}Na nuclides, we compare them, see Appendix C with the iodine radioisotope, ^{131}I, which emits similar radiation (β and γ), and is widely used in the therapy of thyroid cancer [41]. For radiation therapy, one uses the amount of ^{131}I equivalent to the activity ranging from 0.2 to more than 50 GBq [41]. As 4.6 GBq corresponds to 1 μg of the nuclide, one can take 1 μg as a typical mass per procedure with ^{131}I. The same mass of ^{7}Be in the target is necessary to produce 20 Gy per hour in 1 g of tumor in BeNCT (Table 2). The external dose rate at the distance of 1 m from the source, $\dot{D}_{\text{ext}}$, which characterizes the radiation risk for the environment and the personnel, is 2.5 times smaller for ^{7}Be (0.09 mGy/h) than for the typical therapeutic amount of ^{131}I. For ^{22}Na, the necessary mass of the nuclide is 3 μg per 1 g of the tumor, and $\dot{D}_{\text{ext}}$ = 0.21 mGy/h is similar to that of 1 μg of ^{131}I. The β component of the internal spontaneous dose is absorbed locally, within 2 mm from the source. It produces a therapeutic effect in the tumor and is harmful when the radionuclide is in the healthy tissues. In the case of ^{131}I, the internal dose rate is $\dot{D}^{\beta}_{\text{int}}$ = 360 mGy/h for 1 μg of the nuclide; it is eight times lower for 3 μg of ^{22}Na, and it is absent for ^{7}Be. However, the main therapeutic effect of ^{22}Na and ^{7}Be comes from the neutron capture reaction and has an absorbed dose rate of 20 Gy/h, i.e., it is more than 50 times stronger than that for ^{131}I. The γ component of the internal dose is absorbed (by definition) within the sphere of R = 10 cm from the decaying nuclides and, most probably, outside the tumor. Therefore, damages the healthy tissues with the same dose rate of about $\dot{D}^{\text{Y}}_{\text{int}}$ = 60 mGy/h per 1 μg of ^{131}I and 3 μg of ^{22}Na; the effect is 2.5 times smaller for 1 μg of ^{7}Be. Therefore, we conclude that if administered in the same amount as ^{131}I for thyroid cancer therapy (i.e., in the range of micrograms), the radiation risk from spontaneous decay of ^{7}Be and ^{22}Na would be at the same level or smaller than that for ^{131}I. Thus, the nuclides can be managed and administered by following a standard security procedure and technologies for radiopharmaceuticals for radioisotope therapy. However, simultaneously, the therapeutic effect for the tumor is much stronger and with better temporal control for NCT than for the standard radionuclide treatment. The assessment of the radio-toxicity of the nuclides also should take into account their biological halftimes. This issue is strongly connected to the properties of the drug

containing a nuclide, which should control targeting, biodistribution, and pharmacokinetics, as discussed in the following paragraphs.

The major challenge for future NCT research is how to provide the targeting, the accumulation, and the pharmacokinetic timescales for ^{7}Be and ^{22}Na at the same level as in the case of ^{131}I therapy. In other words, one needs a substance that binds the radionuclide, transports it selectively into a specific cancerous tissue providing the nuclide concentration of 1–3 ppm for several hours, and then is excreted together with the remaining non-activated nuclides within several days. Of the total administered amount of several (up to a few tens) micrograms of the nuclide per procedure (the amount limited by the spontaneous radiation risk), a substantial part (more than 10%) should pass through the tumor. The abovementioned limitations of the total amount of the nuclide and the required pharmacokinetics will also eliminate (or substantially ease) the problem of chemical toxicity of the pure elements, and in particular, that for beryllium (the median lethal dose, LD50, for animals is more than 10 mg beryllium/kg [42]). Besides, there is a second criterion, the nuclide accumulation selectivity, arising from the requirement to minimize the radiation risk under neutron irradiation – the ratio of the nuclide concentration in the tumor and in the surrounding healthy tissues must be larger than 3 [15].

The earlier approach employed in the BNCT consists of binding the active nuclide into a soluble enough and low-toxic compound administered in large quantities to achieve the desirable concentration in the target tissue, e.g., boronophenylalanine and sodium borocaptate [14]. However, the tumor targeting for these compounds is not sufficient. For example, one had to administer around 10 mg of boron per 1 kg of the patient's weight [15] to achieve the necessary nuclide concentration in the tumor. Therefore, only a small part of ^{10}B ends up in the tumor, while almost 1 g of that enters the healthy tissues and should be excreted. Obviously, this approach does not fit the BeNCT and NaNCT due to the spontaneous radioactivity. Another method of delivery can be based on recent developments in nanomedicine [14,43] and could be utilized for the new NCT. This modular approach can comprise two or three of the following steps. One first binds the nuclide in a stable compound, then encapsulates it into a nanoparticle having sufficient solubility, pharmacokinetics, and low toxicity, and finally, functionalizes the nanoparticles to target specific cells.

The nanomedicine approach can potentially provide a very high selectivity, and it is especially suitable for NCT. Here, there is no need to release the drug in the target tissues as in the case of chemically acting compounds – the ionizing radiation will exit the nanocage anyway. Moreover, it would be advantageous to keep the non-activated nuclides tightly encapsulated during the whole procedure to eliminate the radiotoxicity risk and control the excretion. A possible way to prevent the nuclide's interaction with the aqueous medium (and thus their toxicity, in particular, beryllium) could be encapsulation in a low-reactivity vessel. Due to their availability and well-studied properties, fullerenes appear as a logical choice but sealed nanotubes could prove useful, as well as derivatives or supramolecular coordination complexes [44,45]. We have shown recently [24,46] that the energetic barrier for beryllium to cross the wall of a C36 fullerene is 1–2 eV, but one may argue that C60 would be a better choice due to its lower reactivity. Then, a poorly soluble fullerene can be functionalized or encapsulated further (into, e.g., a liposome) to improve the pharmacokinetics. From here, we can functionalize the fullerene again to target the specific tissue by following the existing nanomedicine techniques [14,43]. Also, recent developments in beryllium-organic chemistry [47,48] potentially could provide other options for the coordination of beryllium.

Conclusion

We have put forward physical arguments in favor of the potential use of ^{7}Be and ^{22}Na nuclides for neutron capture therapy. We have discussed their advantages vs existing BNCT, limitations, and new challenges arising from the spontaneous radioactivity, and the production issues. The use of new nuclides alone or in combination with traditional ^{10}B and/or ^{157}Gd would open up a new way in neutron capture therapy, unexplored before. There are no other reasonably stable nuclides that have the capture cross section for the thermal and epithermal neutrons larger than that for ^{10}B and emit high LET radiation suitable for NCT. By combining BeNCT and NaNCT with SPECT (or NaNCT with PET), one would obtain real theranostics – simultaneous imaging of the nuclide biodistribution and the targeted therapy of cancerous tissues – an important ingredient of modern personalized medicine.

Acknowledgements: MC and IVB thank Paolo Randaccio for useful discussions, Detlef Gabel for his constructive criticism and suggestions regarding the radiotoxicity issue, and Wolfgang Sauerwein for the critical but encouraging discussions. The authors thank Stefan Milenkovic for his help in the preparation of the manuscript.

Funding information: EVT was supported by a grant from the Russian Science Foundation (Project No. 19-72-30014). This study was funded by bilateral Russian (RFBR) Italian (CNR) research Projects 20-58-7802 (RFBR) and CUP: B55F21000620005 (CNR). We acknowledge a CINECA award under the ISCRA initiative (Project No. IsC92 BeNCTS) for the availability of high performance computing resources and support.

Conflict of interest: The authors state no conflict of interest.

Data availability statement: The datasets generated during and/or analyzed during the current study are available from the corresponding author on reasonable request.

References

[1] Baskar R, Lee KA, Yeo R, Yeoh K-W. Cancer and radiation therapy: Current advances and future directions. Int J Med Sci. 2012;9(3):193–9. doi: 10.7150/ijms.3635.

[2] Citrin DE. Recent developments in radiotherapy. N Engl J Med. 2017;377(11):1065–75. doi: 10.1056/NEJMra1608986.

[3] De Ruysscher D, Niedermann G, Burnet NG, Siva S, Lee AWM, Hegi-Johnson F. Radiotherapy toxicity. Nat Rev Dis Prim. 2019;5(1):13. doi: 10.1038/s41572-019-0064-5.

[4] Ziegler JF, Biersack J, Littmark U. The stopping and range of ions in solids. New York: Pergamon; 1985.

[5] Mitin T, Zietman AL. Promise and pitfalls of heavy-particle therapy. J Clin Oncol. 2014;32(26):2855–63. doi: 10.1200/JCO.2014.55.1945.

[6] Newhauser WD, Zhang R. The physics of proton therapy. Phys Med Biol. 2015;60(8):R155–209. doi: 10.1088/0031-9155/60/8/R155.

[7] Terasawa T. Systematic review: Charged-particle radiation therapy for cancer. Ann InternMed. 2009;151(8):556. doi: 10.7326/0003-4819-151-8-200910200-00145.

[8] Jadvar H. Targeted radionuclide therapy: An evolution toward precision cancer treatment. Am J Roentgenol. 2017;209(2):277–88. doi: 10.2214/AJR.17.18264.

[9] Locher GL. Biological effects and therapeutic possibilities of neutrons. Am J Roentgenol. 1936;36:1–13.

[10] Farr L, Sweet W, Locksley H, Robertson J. Neutron capture therapy of gliomas using boron. Trans Am Neurol Assoc. 1954;13(79th Meeting):110.

[11] Barth RF, Coderre JA, Vicente MGH, Blue TE. Boron neutron capture therapy of cancer: current status and future prospects. Clin Cancer Res. 2005;11(11):3987–4002. doi: 10.1158/1078-0432.CCR-05-0035.

[12] Barth RF, Vicente MH, Harling OK, Kiger W, Riley KJ, Binns PJ, et al. Current status of boron neutron capture therapy of high grade gliomas and recurrent head and neck cancer. Radiat Oncol. 2012;7(1):146. doi: 10.1186/1748-717X-7-146.

[13] Slatkin DN, Javid MJ, Joel DD, Kalef-Ezra JA, Ma R, Feinendegen LE. A history of 20th-century boron neutron-capture therapy. J Neurol Neurobiol. 2017;3(2). doi: 10.16966/2379-7150.142.

[14] Barth RF, Mi P, Yang W. Boron delivery agents for neutron capture therapy of cancer. Cancer Commun. 2018;38(1):35. doi: 10.1186/s40880-018-0299-7.

[15] Moss RL. Critical review, with an optimistic outlook, on boron neutron capture therapy (bnct). Appl Radiat Isot. 2014;88:2–11. doi: 10.1016/j.apradiso.2013.11.109.

[16] Cerullo N, Bufalino D, Daquino G. Progress in the use of gadolinium for nct. Appl Radiat Isot. 2009;67(7–8 SUPPL):157–60. doi: 10.1016/j.apradiso.2009.03.109.

[17] Enger SA, Giusti V, Fortin M-A, Lundqvist H, af Rosenschöld PM. Dosimetry for gadolinium neutron capture therapy (gdnct). Radiat Meas. 2013;59:233–40. doi: 10.1016/j.radmeas.2013.05.009.

[18] Deagostino A, Protti N, Alberti D, Boggio P, Bortolussi S, Altieri S, et al. Insights into the use of gadolinium and gadolinium/boron-based agents in imaging-guided neutron capture therapy applications. Future Med Chem. 2016;8(8):899–917. doi: 10.4155/fmc-2016-0022.

[19] Jin WH, Seldon C, Butkus M, Sauerwein W, Giap HB. A review of boron neutron capture therapy: Its history and current challenges. Int J Part Ther. 2022;9(1):71–82. arXiv . doi: 10.14338/IJPT-22-00002.1. https://meridian.allenpress.com/theijpt/article-pdf/9/1/71/3077901/i2331-5180-9-1-71.pdf.

[20] Tilley D, Cheves C, Godwin J, Hale G, Hofmann H, Kelley J, et al. Energy levels of light nuclei *A*=5,6,7. Nucl Phys A. 2002;708(1–2):3–163. doi: 10.1016/S0375-9474(02)00597-3.

[21] Basunia MS. Nuclear data sheets for *A*=59. Nucl Data Sheets. 2018;151:1–333. doi: 10.1016/j.nds.2018.08.001.

[22] Segre E. Minutes of the meeting at los angeles, California: january 3-4, 1947. Phys Rev. 1947;71:274–9. doi: 10.1103/PhysRev.71.274.

[23] Daudel R. Alterations des periodes radioactives sous l'influence des methodes chimiques. Rev Sci. 1947;85:162.

[24] Tkalya EV, Avdeenkov AV, Bibikov AV, Bodrenko IV, Nikolaev AV. Electron capture β decay of ^{7}Be located inside and outside the C_{36} fullerene. Phys Rev C. 2012;86:014608. doi: 10.1103/PhysRevC.86.014608.

[25] Cyburt RH, Fields BD, Olive KA, Yeh T-H. Big bang nucleosynthesis: Present status. Rev Mod Phys. 2016;88:015004. doi: 10.1103/RevModPhys.88.015004.

[26] Damone L, Barbagallo M, Mastromarco M, Mengoni A, Cosentino L, Maugeri E, et al. Zugec, ˇ ^{7}Be(n,p)^{7}Li reaction and the cosmological lithium problem: measurement of the cross section in a wide energy range at n TOF at CERN. Phys Rev Lett. 2018;121(4):42701. doi: 10.1103/physrevlett.121.042701.

[27] Koehler PE, O'Brien HA. ^{22}Na(n,p)^{22}Ne and ^{22}Na(n,α)^{19}F cross sections from 25 meV to35 keV. Phys Rev C. 1988;38(5):2019–25. doi: 10.1103/PhysRevC.38.2019.

[28] Evaluated nuclear data file (endf). https://www.nndc.bnl.gov/endf/. https://www.nndc.bnl.gov/endf/.

[29] Carlson A, Pronyaev V, Capote R, Hale G, Chen Z-P, Duran I, et al. Evaluation of the neutron data standards. Nucl Data Sheets. 2018;148:143–88. doi: 10.1016/j.nds.2018.02.002.

[30] Tomandl I, Vacík J, Köster U, Viererbl L, Maugeri EA, Heinitz S, et al. Measurement of the ^{7}Be(n,p) cross section at thermal energy. Phys Rev C. 2019;99(1):3–8. doi: 10.1103/PhysRevC.99.014612.

[31] Koehler PE, Bowman CD, Steinkruger FJ, Moody DC, Hale GM, Starner JW, et al. ^{7}Be(n,p)^{7}Li total cross section from 25 meV to 13.5 keV. Phys Rev C. 1988;37(3):917–26. doi: 10.1103/PhysRevC.37.917.

[32] Berger MJ, Coursey JS, Zucker MA, Chang J. Stopping-power and range tables for electrons, protons, and helium ions. NIST Standard Reference Database 124; 2017. doi: 10.18434/T4NC7P.

[33] Northcliffe L, Schilling R. Range and stopping-power tables for heavy ions. At Data Nucl Data Tables. 1970;7(3–4):233–463. doi: 10.1016/S0092-640X(70)80016-X.

[34] Busse PM, Harling OK, Palmer MR, Kiger WS, Kaplan J, Kaplan I, et al. A critical examination of the results from the Harvard-MIT

NCT program phase I clinical trial of neutron capture therapy for intracranial disease. J Neurooncol. 2003;62(1):111–21. doi: 10.1023/A:1023249224364.

[35] Kiyanagi Y. Accelerator-based neutron source for boron neutron capture therapy. Ther Radiol Oncol. 2018;2(1):55. doi: 10.21037/tro.2018.10.05.

[36] Anderson I, Andreani C, Carpenter J, Festa G, Gorini G, Loong C-K, et al. Research opportunities with compact accelerator-driven neutron sources. Phys Rep. 2016;654:1–58. doi: 10.1016/j.physrep.2016.07.007.

[37] Patton JA, Turkington TG. SPECT/CT physical principles and attenuation correction. J Nucl Med Technol. 2008;36(1):1. doi: 10. 10.2967/jnmt.107.046839.

[38] Hanaoka K, Watabe T, Naka S, Kanai Y, Ikeda H, Horitsugi G, et al. FBPA PET in boron neutron capture therapy for cancer: prediction of ^{10}B concentration in the tumor and normal tissue in a rat xenograft model. EJNMMI Res. 2014;4(1):70. doi: 10.1186/s13550-014-0070-2.

[39] Maugeri E, Heinitz S, Dressler R, Barbagallo M, Ulrich J, Schumann D, et al. Preparation and characterization of three ^{7}Be targets for the measurement of the ^{7}Be(n,p)^{7}Li and ^{7}Be(n,α)^{7}Li reaction cross sections. Nucl Instrum Methods Phys Res A Accel Spectrom Detect Assoc Equip. 2018 Jan;889:138–44. doi: 10.1016/j.nima.2018.01.078.

[40] Bayanov B, Belov V, Bender E, Bokhovko M, Dimov G, Kononov V, et al. Accelerator-based neutron source for the neutron-capture and fast neutron therapy at hospital. Nucl Instrum Methods Phys Res A Accel Spectrom Detect Assoc Equip. 1998;413(2–3):397–426. doi: 10.1016/S0168-9002(98)00425-2.

[41] Rubino C, de Vathaire F, Dottorini ME, Hall P, Schvartz C, Couette JE, et al. Second primary malignancies in thyroid cancer patients. Br J Cancer. 2003;89(9):1638–44. doi: 10.1038/sj.bjc.6601319.

[42] Toxicological profile for beryllium. ATSDR report. https://www.atsdr.cdc.gov/substances/index.asp.

[43] Tran S, DeGiovanni P-J, Piel B, Rai P. Cancer nanomedicine: a review of recent success in drug delivery. Clin Transl Med. 2017;6(1):44. doi: 10.1186/s40169-017-0175-0.

[44] Dummert SV, Saini H, Hussain MZ, Yadava K, Jayaramulu K, Casini A, et al. Cyclodextrin metal–organic frameworks and derivatives: recent developments and applications. Chem Soc Rev. 2022;51:5175–213. doi: 10.1039/D1CS00550B.

[45] Moreno-Alcántar G, Casini A. Bioinorganic supramolecular coordination complexes and their biomedical applications. FEBS Lett. 2023;597:191–202. arXiv doi: 10.1002/1873-3468.14535.

[46] Bibikov AV, Avdeenkov AV, Bodrenko IV, Nikolaev AV, Tkalya EV. Theoretical study of the pressure effect on the electron-capture β decay of ^{7}Be in ^{7}BeO and ^{7}Be(OH)$_2$. Phys Rev C. 2013;88(3):034608. doi: 10.1103/PhysRevC.88.034608.

[47] Perera LC, Raymond O, Henderson W, Brothers PJ, Plieger PG. Advances in beryllium coordination chemistry. Coord Chem Rev. 2017;352:264–90. doi: 10.1016/j.ccr.2017.09.009.

[48] Iversen KJ, Couchman SA, Wilson DJ, Dutton JL. Modern organometallic and coordination chemistry of beryllium. Coord Chem Rev. 2015;297–298:40–8. doi: 10.1016/j.ccr.2014.11.008.

[49] Cell biology by the numbers. http://book.bionumbers.org/how-big-is-a-human-cell/.

[50] X-ray mass attenuation coefficients, NIST database. https://physics.nist.gov/PhysRefData/XrayMassCoef/tab4.html.

[51] Unger LM, Trubey D. Specific gamma-ray dose constants for nuclides important to dosimetry and radiological assessment. Tech. rep. TN (USA): Oak Ridge National Lab; 1982.

Appendix A

Typical cell size and mass

The average volumes of human cells range from 30 to 4×10^6 μm^3, depending on the tissue [49]; the corresponding linear dimensions range from 3 to 160 μm. For the estimates, we will assume the typical cancer cell volume, V_{cell} = 2,300 μm^3, and the typical cell linear dimension, L_{cell} = 13 μm, which corresponds to HeLa cells often used in cancer *in vitro* studies [49]. Then, we assume the mass density of the cell, ρ_{cell} = 1 g cm^{-3}, so that the typical cancer cell's mass, M_{cell} = 2.3 ng.

Appendix B

Estimation of the absorbed radiation dose under neutron irradiation

The dose of high LET radiation absorbed in a cell is given by $D = E_t N_r / M_{cell}$, where N_r is the number of neutron capture reactions occurring. Thus, the required N_r to release the absorbed radiation dose D locally into the cell is $N_r = DM_{cell}/E_t$. Here, we underline again that we have assumed that the γ-radiation after neutron capture has a small probability to interact and ionize matter within the tumor region (<10 cm) so that the locally deposed energy is only that of the charged particles, E_t. The corresponding estimates for the BNCT, the BeNCT, and the NaNCT are shown in Table 2, assuming D = 20 Gy in tumor tissues for a typical dose required for the radiation therapy in a single run [5,11].

The absorbed dose rate in a cell under a constant neutron flux Φ_n is $\dot{D}(t) = E_t \dot{N}(t)/M_{cell}$, where $\dot{N}(t) = N_0 \exp(-t/\tau_n)/\tau_n$ is the number of the neutron capture reactions in the cell per second, N_0 is the initial (at t = 0) number of nuclide particles per cell; $\tau_n = 1/(\sigma_n J_n)$ is the reaction time constant; and σ_n is the neutron capture cross section. For typical values of σ_n (Table 1) and of the neutron flux, $\Phi_n < 10^{13}$ s^{-1} cm^{-2}, the reaction time constant ($\tau_n > 10^6$ s) is much larger than the reasonable duration of the NCT procedure (up to a few hours). Therefore, if N_0 is not changing significantly during the neutron irradiation procedure due to the accumulation and the excretion, the dose rate is time-independent, and the absorbed dose for time t of the neutron exposure is given by $D(t) = tE_t N_0 \sigma_n J_n / M_{cell}$. Then, the number of nuclides per cell to have the absorbed dose D while exposing for time t to neutron flux Φ_n is $N_{cell} = N_r/(t\sigma_n J_n)$. The corresponding required mass concentration of the nuclide, $c \equiv M$ (nuclide)$/M_{cell}$, is $c = D\mu/(E_t N_A \sigma_n J_n t)$, where μ is the molar mass of the nuclide and N_A is the Avogadro constant. In Table 2, we show the estimated concentration of nuclide (both N_{cell} and c) required to obtain the absorbed radiation dose of D = 20 Gy in water after 1 h exposure to $\Phi_n = 10^{10}$ s^{-1} cm^{-2} neutron flux for thermal and epithermal neutron energies.

Once the neutrons enter the target (a water phantom or a human body) with initial energy E_n^0, they start to scatter on the atoms (mainly, elastically and on hydrogens) and slow down. The average neutron energy in the target, $E_n(x)$, decreases with the depth x from the initial energy $E_n(0)$ at x = 0 until the thermal energy is equal to $3/2k_BT$ at a given temperature T, and the neutron capture cross section is $\sigma_n(E_n(x))$, for the active nuclide increases with x reaching the value for the thermal neutrons. Besides, neutrons change their direction after each collision so that the initially collimated beam will disperse with the distance traveled in the target. Therefore, the neutron flux $\Phi_n(x)$ along the initial beam direction decreases with the depth x. As the absorbed dose is proportional to the product, $D(x) \propto \sigma_n(E_n(x))J_n(x)$, it also depends on the depth x even at a uniform concentration of the active nuclide. If the incident neutrons are already thermalized, their average energy and the capture cross section are constant so that the dose decreases with the depth due to the decrease of the average flux. If the initial neutrons have a higher energy (0.5 eV to 10 keV), the absorbed dose, $D(x)$, first increases with x together with the neutron capture cross section, then reaches its maximum at a certain distance x_0 (1–4 cm) [35], and then decreases due to the flux angular dispersion. The interval of the depth, $[x_{min}, x_{max}]$ around x_0, where the absorbed dose is higher than a certain critical value (e.g., 20 Gy/h) at a given nuclide concentration is suitable for the NCT. For the ^{7}Be and the ^{22}Na nuclides, having the neutron capture cross section larger than that for ^{10}B by a factor of 10, the maximum working depth, x_{max}, can be much larger than x_0 and can reach 10–20 cm required for potential therapy of deep sitting tumors.

Appendix C

The absorbed dose from the spontaneous radiation

To estimate the effects of the spontaneous radiation of ^{7}Be and the ^{22}Na nuclides, both for the patient and for the personnel, we compare them with the iodine radioisotope, ^{131}I, which emits similar radiation and also is widely used in the

Table A1: Comparison of the radiation effects of the spontaneous decay

Nuclide (half-life)		
^{131}I (8.0 d)	^{7}Be (53 d)	^{22}Na (2.60 y)
Mass-specific activity, A_m [GBq/μg] radiation type, its energy, and the abundance		
4.6	13	0.23
γ, 370 keV (average)	γ, 478 keV, f = 0.10	γ, 1,280 keV, f = 1
β^-, 570 keV (average)		β^+, 540 keV, f = 0.9, γ, 511 keV, f = 1.8
γ constant at a distance of 1 m, Γ [mGy/h/GBq]		
0.05	0.007	0.30
External absorbed dose rate, $\dot{D}_{ext}$ [mGy/h] per 1 μg of nuclide at a distance of 1 m		
0.23	0.09	0.07
Internal absorbed dose rate per 1 μg of nuclide, $\dot{D}_{int}$ [mGy/h] contribution for each radiation type is specified separately		
60 – γ	25 – γ	18 – γ
360 – β		15 – β
Total: 420		Total: 33

therapy of thyroid cancer [41] (Table A1). There are several standard physical characteristics of spontaneous decay.

Iodine isotope has the shortest lifetime, $T_{1/2}$, of 8 days, while the sodium isotope's half-life is the longest among the three nuclides and equals 2.6 years. The activity of a radionuclide (the number of decays per second) of initial mass M, after time t is

$$A(t) = A_m M \exp\left(-\ln(2)\frac{t}{T_{1/2}}\right), \tag{C1}$$

where $A_m = \ln(2)N_A/(\mu T_{1/2})$ is the nuclide-mass-specific activity and μ is the molar mass. Table A1 shows that the mass-specific activity for ^{7}Be is the largest despite the half-life for ^{131}I being shorter; apparently, it is due to the almost 20 times larger isotope mass for the iodine.

To characterize the external (personnel and environmental) radiation risk of a radionuclide, one usually calculates the absorbed radiation dose rate at a certain distance d from a point-like source of activity A. The distance is typically large enough (e.g., 1 m) so that all the β radiation is absorbed well before d, and only γ-radiation contributes to the ionization. The external γ-radiation dose rate is given as

$$\frac{dD_{ext}}{dt} = \Gamma\frac{A}{d^2}P_s. \tag{C2}$$

Here, the γ constant,

$$\Gamma = \frac{1}{4\pi}\frac{\mu_{en}}{\rho}\sum_i E_\gamma^i f^i \tag{C3}$$

is a standard characteristic of the external radiation risk of the nuclide at a given activity. The sum in the latter equation runs over the energies of all the emitted γ particles weighted by the corresponding abundance (f^i is the average number of photons of type i per decay of the nuclide). The energy attenuation coefficient, μ_{en}, determines the average relative energy loss of the photon beam after passing distance x in the material: $E/E_0 = \exp(-\mu_{en}x)$. As μ_{en} is approximately proportional to the mass density, ρ, of the material, one often introduces the mass-energy attenuation coefficient, μ_{en}/ρ. In particular, for both air and liquid water, $\mu_{en}/\rho \approx 0.03$ cm^2 g^{-1} with 20% accuracy for the photon energies from 60 keV to 2 MeV [50]. The γ shielding factor, P_s, describes the reduction of the average energy of the emitted photons due to the absorption and the inelastic scattering on the way from the source to the observation point at a distance d. If the energy attenuation coefficient of the shielding material, as discussed above, μ_{en}^s, weakly depends on the photon energy. The shielding factor can be estimated as follows: $P_s = \exp(-\mu_{en}^s L)$, where $L \le d$ is the thickness of the shield. In air, $\rho_s = 0.001225$ g cm^{-3}, and the characteristic energy attenuation length, $\lambda = 1/\mu_{en}^s$ is about 270 m so that at a distance below d = 1 m, the shielding factor, $P_s = \exp(-d/\lambda) \approx 1$. The energies and the corresponding abundances of the radiation are shown in Table A1. For ^{131}I, more than 10 different photons may be emitted [51], and we show only the average (weighted) value, $\sum_i E_\gamma^i f^i$, in the table. The calculated Γ constants reported in Table A1 agree with the values recommended in the study of Unger and Trubey [51] within 20% accuracy sufficient for the nuclide comparison presented here. This also justifies the approximations accepted for the simplified estimates of the absorbed doses. The calculated external dose rate at 1 m per 1 μg of nuclide, $\dot{D}_{ext}$, is reported in Table A1.

To quantify the possible effect of the spontaneous radiation on the patient, we calculate the average absorbed dose rate within a sphere of water of radius R = 10 cm around a pointlike source. The β-radiation from the spontaneous decay is completely absorbed within less than 2 mm from the source [32], releasing the energy, $P_i E_\beta^i f_\beta^i$. The photons, on average, lose only a part of their initial energy equal to $(1 - \exp(-\mu_{en}R))\sum_i E_\gamma^i f^i$. The internal absorbed dose rate is the sum of the two contributions:

$$D_{int} = D_{int}^\gamma + D_{int}^\beta, \tag{C4}$$

$$\frac{dD_{int}^\gamma}{dt} = A(1 - \exp(-\mu_{en}R))\sum_i E_\gamma^i f^i \frac{3}{4\pi R^3\rho}$$
$$\frac{dD_{int}^\beta}{dt} = A\sum_i E_\beta^i f_\beta^i \frac{3}{4\pi R^3\rho} \tag{C5}$$

The calculated external dose rate per 1 μg of nuclide, $\dot{D}_{\text{int}}$, is reported in Table A1 for the photons and the β-particles, separately.

The half-life, the mass-specific activity, and the Γ constant reflect different physical properties of radioactive nuclides, and, separately, are not sufficient to characterize the risk of spontaneous radiation. The mass-specific internal $\dot{D}_{\text{int}}$ and external, $\dot{D}_{\text{ext}}$, dose rates defined here are more suitable for comparing radionuclides.

For the radiation therapy of thyroid cancer, one uses the amount of ^{131}I equivalent to the activity ranging from 0.2 to >50 GBq [41]. As 4.6 GBq corresponds to 1 μg (Table A1) of the nuclide, we can consider 1 μg as a typical mass per procedure with ^{131}I. The same mass of ^{7}Be in the target would be necessary to produce 20 Gy per hour in 1 g of tumor in BeNCT (Table 2). The external dose rate at 1 m, $\dot{D}_{\text{ext}}$, characterizing the radiation risk for the environment and the personnel, is 2.5 times smaller for ^{7}Be (0.09 mGy/h) than for the typical therapeutic amount of ^{131}I. For ^{22}Na, the necessary mass of the nuclide is 3 μg per 1 g of tumor, and $\dot{D}_{\text{ext}}$ = 0.21 mGy/h is similar to that of 1 μg of ^{131}I.

The β component of the internal spontaneous dose is absorbed locally. It produces a therapeutic effect in the tumor and it is harmful when the radionuclide is in the healthy tissues. In the case of ^{131}I, the dose rate is $\dot{D}_{\text{int}}^{\beta}$ = 360 mGy/h for 1 μg of the nuclide. It is 8 times lower for 3 μg of ^{22}Na and it is absent for ^{7}Be. However, the therapeutic effect of ^{22}Na and ^{7}Be comes from the neutron capture reaction and has an absorbed dose rate of 20 Gy/h, i.e., it is more than 50 times stronger than for ^{131}I.

The γ component of the internal dose is absorbed (by definition) within the sphere of R = 10 cm from the decaying nuclides, and most probably, outside the tumor. Therefore, it makes the radiation damage to healthy tissues with the same dose rate of about $\dot{D}_{\text{int}}^{\Upsilon}$ =60 mGy/h per 1 μg of ^{131}I or 3 μg of ^{22}Na; the effect is 2.5 times smaller for 1 μg of ^{7}Be.